NMR Studies of Structural Phase Transitions in Random Copolymers

Mark McCormick*,† and Jeffrey A. Reimer

Lawrence Berkeley National Laboratory and Department of Chemical Engineering, University of California, Berkeley, California 94720

Received September 4, 2002; Revised Manuscript Received November 13, 2002

ABSTRACT: Nuclear magnetic resonance (NMR) has been used in conjunction with circular dichroism (CD) and intrinsic viscosity (IV) measurements to probe the phase diagram of poly(L-glutamic acid-*ran*-L-leucine) (PEL). IV measurements indicate that PEL in aqueous salt solution undergoes a pH-mediated collapsing transition whereby its size decreases by a factor of 2.6 as the pH is decreased from 6.82 to 4.92. CD measurements indicate a pH-mediated helix−coil transition as the pH is increased from less than 5 to greater than 7. NMR relaxation times and nuclear Overhauser effects were obtained as a function of temperature for various phases of the PEL system and analyzed according to various models for polymer dynamics. The results of these analyses are discussed in the context of freezing transitions predicted by contemporary theories of random copolymers.

Introduction

Polymer theorists have modeled the folding of proteins by using computational and analytical methods based on the behavior of random copolymers. For example, it has been postulated that random copolymers, under the proper conditions, will undergo a "freezing transition" from a Gaussian coillike state to a phase where the chain will be dominated by a few conformations (of order 1). These analytical theories and computational models have resulted in the specific prediction that random copolymers of carefully selected monomers (approximately 2−3) that interact differently with the solvent and each other can lead to "collapsed" and "frozen" phases.[1]

The freezing transition is thought to result from enthalpic frustration of the random copolymer. Consider a two-letter random copolymer of monomer types A and B that interacts unfavorably; chemical connectivity of the A and B monomers precludes their phase separation. To minimize chain free energy, the system undergoes a microphase separation forming small (compared to the size of the globule) A-rich and B-rich domains. Even if a rearrangement is attempted, for example when an A unit migrates from a B-rich domain to an A-rich domain, connectivity requires accompaniment of the unfavorable unit, resulting in the creation of many more unfavorable interactions than favorable interactions. Such migrations and associated chain rearrangements therefore face extremely high activation energies and rarely occur. The result is a "frozen" polymer globule with minimal multisegmental motion.

The frozen phase of a polymer chain is characterized by a restricted conformational space, exchanging entropic free energy for discrete low enthalpic states.[2] Figure 1 depicts the energy density of states for "stiff" and "flexible" random copolymer chains. At low energies, the density of states decreases to the point where the number of conformations is of order 1 (meaning that the entropy is nearly 0). The transition from the continuum of states to the discrete states is the freezing transition.[2]

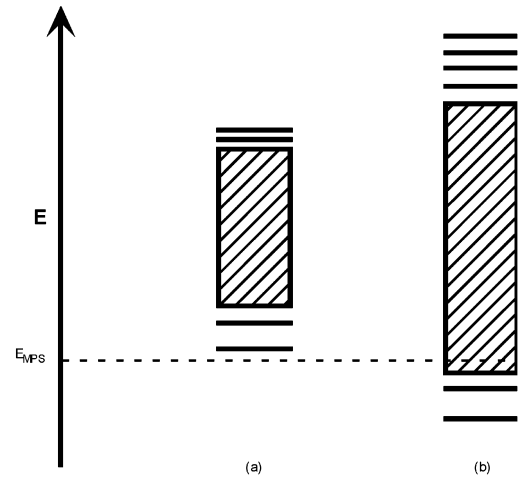

Figure 1. Energy diagram showing the density of states of a stiff (a) and flexible (b) chain. E_{MPS} is the energy where microphase separation occurs. The hatched box represents a continuum of states. Adapted from ref 2.

Detection and characterization of the freezing transition for random polymers differ from protein folding in one very important way. Consider the random energy model[3] that has been useful in describing the kinetics and thermodynamics of protein folding. This model manipulates the energy landscape to have one single deep minimum with a large amount of funneling.[4] Conformation-specific techniques, such as X-ray crystallography and multidimensional NMR, are useful for characterizing the low-energy state (single conformation) if the polymer chains have identical sequences and uniform molecular weights (e.g., proteins). For the case of statistical random copolymers, however, each chain has a different sequence, thus experiencing a different energy landscape. In the case of statistical polymers with significant sequence variability and polydispersity, there is not a single conformation common to most chains; therefore, the *dynamics* of the ensemble of chains must be used to detect the freezing transition.

Finally, the freezing transition can be contrasted with "collapsing transitions". These transitions are solvent-mediated and reflect a preference for the polymer segments to associate with themselves as opposed to the

* To whom correspondences should be addressed. E-mail mccormic@mpip-mainz.mpg.de.

† Current address: Max Planck Institute for Polymer Research, Postfach 3148, 55118 Mainz, Germany.

10.1021/ma021433k CCC: $25.00
Published on Web 12/21/2002

solvent. The uncollapsed (coil) state "breathes" as the coil explores all of its possible conformations; the fluctuations of the density (size) of the polymer coil are on the order of its own density (size). In the collapsed state, the fluctuations of density and size are much smaller; however, the chain can still sample many conformations. The transition from an uncollapsed to a collapsed state has been studied extensively in homopolymers such as poly(styrene) dissolved in cyclohexane[5] and poly(acrylic acid) dissolved in dioxane.[6] Furthermore, many authors have produced phase diagrams that describe the behavior of chains in solution.[1,2] One such diagram predicts three phases.[1] For good solvents, the chain exists in a homopolymer-like random coil, regardless of chemical heterogeneity. In poor solvents, chains with little heterogeneity exist as a homopolymer-like random globule, which is a collapsed state that samples all conformations. If a heterogeneous chain is in a poor solvent, the chain will be in a frozen globule.

This work endeavors to experimentally probe the phase diagram of a commercially prepared random copolymer. We utilize intrinsic viscosity to probe the collapsing transition, circular dichroism to probe the helix−coil transition, and NMR to probe the dynamics of the polymer chains. The results of these analyses are discussed in the context of the freezing transitions predicted by contemporary theories.

Experimental Section

Materials. The copolymer poly(L-glutamic acid-*ran*-L-leucine) (PEL) was purchased as a sodium salt from Sigma Chemical Co. (St. Louis, MO). It contains 17% L-leucine and has a number-average molecular weight of 60 200 Da, corresponding to a degree of polymerization (DP) of 420; the polydispersity index (PDI) is given as 1.46. This sample was chosen because it has been shown to exist in many aqueous environments in a nonaggregated state.[7−11] Poly(L-glutamic acid) (PLGA) was also purchased as the sodium salt (Sigma) and is reported to have a number-average molecular weight of 61 200 Da, corresponding to a DP of 405 with a PDI of 1.3.

Viscosity Measurements. Viscosity measurements were carried out with a Schott Geräte dilution capillary viscometer, utilizing a Schott AVS 350 controlled by an AT&T 6312WL computer to record the times. Temperature was maintained to ±0.1 °C by immersing the viscometer in a Neslab RTE110 constant-temperature bath. Dilutions were carried out by the addition of buffer to the viscometer, with concentrations determined by weighing the sample before and after each dilution. The flow is monitored by an optical detector that can detect the meniscus interface between the sample and air.

Circular Dichroism Measurements. Circular dichroism measurements were carried out at room temperature on a Jasco J-600 spectropolarimeter using 1 cm path length stress-free quartz cylindrical cells. The resulting spectra were digitized at 0.2 nm per point with a bandwidth of 1.0 nm, a time constant of 8 s, and a sweep rate of 5 nm/min. The samples were prepared by starting with solution aliquots with polymer concentrations of 0.015 mg/mL; the pH was then adjusted via addition of phosphoric acid or potassium hydroxide, and the final concentration was calculated after weighing the samples. The pH was measured again after the spectra were taken and were always within 0.01 pH units of the original measurement. Data were obtained in solutions of phosphate buffer with 0.02 M KH_2PO_4 and 0.2 M KF, which resulted in a Debye length of 6.78 Å.

Nuclear Magnetic Resonance Measurements. NMR experiments were carried out on a home-built 300 MHz dual-channel spectrometer utilizing a Tecmag Libra pulse programmer. The samples were contained in 5 mm tubes (Wilmad Glass), and spectra were acquired with a Cryomagnetics liquids probe. Temperature was controlled via an Omega Engineering temperature controller and flowing air or nitrogen gas. The carbon frequency was 75.57 MHz. Proton spectra, DQF−COSY, heteronuclear correlation, and DEPT spectra were used to aid in resonance assignment.

Spin−lattice relaxation times, spin−spin relaxation times, and $^{13}C\{^1H\}$ NOEs were measured for PEL in buffered solution at pH 4.58 and pH 7.10 for temperatures of 25, 45, and 65 °C. PEL samples were prepared from polymer dissolved previously in D_2O and subsequently lyophilized. Buffered solutions prepared from 0.2 M KCl and 0.02 M KD_2PO_4 in D_2O were filtered through 0.22 μm membrane filters; one was adjusted to a pH of 4.58 with phosphoric acid and the other adjusted to a pH of 7.10 with KOH. 24 mg of the exchanged PEL was dissolved in 600 μL of these buffer solutions, then sonicated for 30 min, and subsequently centrifuged at 12 000 rpm for 5 min to remove insolubles. The pH of the solutions was checked and adjusted as necessary.

Relaxation times were measured using the inversion recovery and CPMG[12] methods. NOE's were determined by dividing the integral of a ^{13}C peak acquired with proton irradiation by the integral of a peak acquired with gated decoupling of the protons. Proton irradiation (10 kHz bandwidth) was accomplished with a broadband decoupler set at 300 MHz.

Results

Intrinsic Viscosity. The intrinsic viscosity measurements (Table 1) can be used to estimate the size of the globule. The data in Table 1 yield a collapsing ratio of 2.6 when the pH is changed from 4.92 to 6.82. This is consistent with size exclusion chromatography data reported previously[11] as well as intrinsic viscosity data for proteins of a similar molecular weight.[13]

Circular Dichroism. The CD data show pH-mediated secondary structure transitions, as seen by the full spectra for a PEL sample in buffered solutions of varying pH (Figure 2). At low pH the sample shows the characteristic double minima at 208 and 222 nm. At higher pH, the sample displays a maximum at 218 nm and a minimum at about 198 nm. Each spectrum was deconvoluted in terms of a basis set of spectra for α-helix, β-strand, and random coil, resulting in a ratio

Table 1. Measured Intrinsic Viscosity Data for PEL[a]

temp (K)	pH	$[\eta]$ (mL/g)	$\langle s^2\rangle^{1/2}$ (nm)
298	4.92	3.99	2.61
298	5.01	5.47	2.90
298	6.52	52.4	6.15
298	6.82	69.0	6.75
318	4.91	8.53	3.36

[a] $\langle s^2\rangle^{1/2}$ is calculated using Einstein's definition of intrinsic viscosity of a solution of hard spheres.[14]

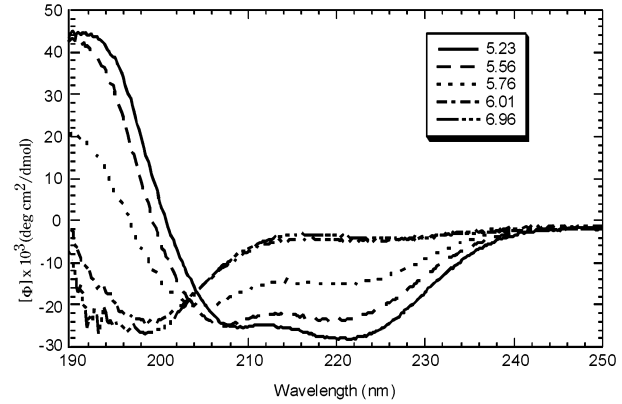

Figure 2. Circular dichroism spectra for poly(L-glutamic acid-*ran*-L-leucine) at various pHs.

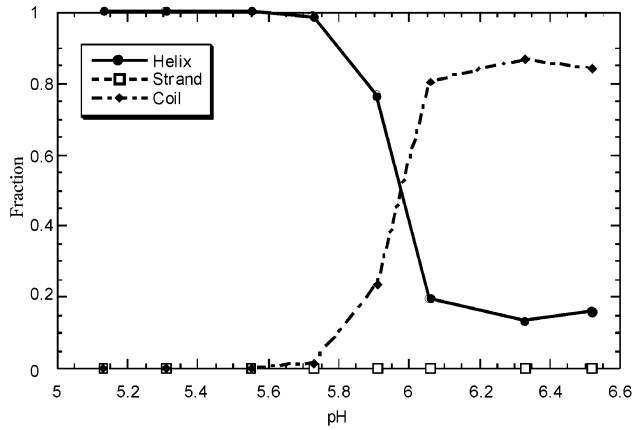

Figure 3. Fraction of poly(L-glutamic acid) in α-helix, *β*-strand, and random coil as a function of pH.

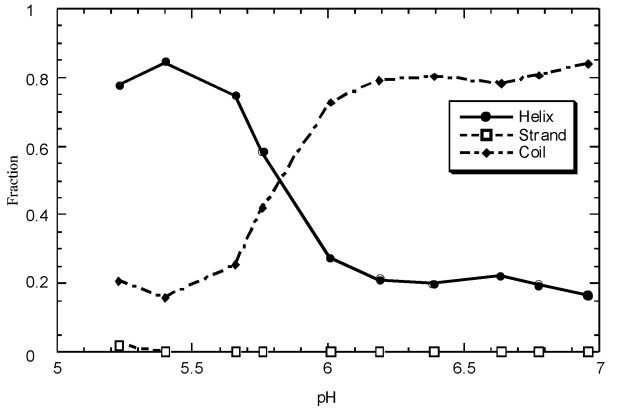

Figure 4. Fraction of poly(L-glutamic acid-*ran*-L-leucine) in α-helix, *β*-strand, and random coil as a function of pH.

of structural types. The transition pH is determined by the intersection of the interpolated fractional helix and coil curves. PLGA displays a helix−coil transition at pH 5.95 (Figure 3), and PEL exhibits a helix−coil transition at pH 5.83 (Figure 4).

It has been shown that PLGA experiences an apparent pK_a shift to higher values when in solution.[8] In 0.2 M salt solutions, the pK_a of the glutamic acid residues on PLGA is approximately 5.15; therefore, the average charge per monomer at the helix−coil transition is −0.85. On PEL this would correspond to an average charge per monomer at the helix−coil transition of −0.66 (79% of glutamic acid residues carry a charge).

Nuclear Magnetic Resonance Peak Assignments. NMR peaks were assigned on the basis of previously reported chemical shifts[15] and were confirmed via double-quantum-filtered correlation spectroscopy (DQF-COSY).[16] Single-pulse ^{13}C spectra were collected for both high- and low-pH systems at 25, 45, and 65 °C. The literature[17] and the DEPT experiments aided peak assignment. A heteronuclear correlation experiment[18] was also run to confirm the preliminary assignments.

Peak assignments are reported in Table 2. The Glu *γ* carbon was assigned to two resonances: one at 34.5 ppm is assigned to a Glu *γ* carbon on an unprotonated side chain; the other at 31.2 ppm corresponds to a Glu *γ* carbon on a protonated side chain (designated Glu γ_H). Multiple resonances are predicted for the other glutamic acid carbons as well. The Glu α, Glu *β*, and backbone carbonyl line widths, however, are so broad as to make the peaks indistinguishable. The side chain carbonyl

Table 2. Chemical Shifts for Protons and Carbons in the PEL Random Copolymer

	glutamic acid[a,b]		leucine[b]	
position	carbon-13	proton	carbon-13	proton
α	54.6	4.45	53.2	4.20
β	28.9	2.05, 2.10	40.7	1.75
γ	34.5 (31.2)	2.3, 2.45 (2.5)	25.3	1.30
δ_1, δ_2			23.2, 21.8	0.95, 0.90

[a] Parenthetical chemical shift reported for Glu *γ* is for a protonated glutamic acid residue. [b] Multiple entries indicate multiple peaks assigned to the same position.

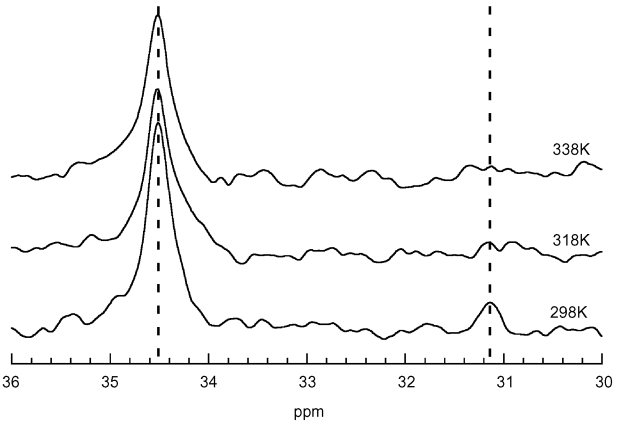

Figure 5. Carbon-13 spectra of the Glu *γ* region at pH 4.58. The dotted lines are an aid to the eye.

does display a protonated peak; however, the long relaxation time of the carbonyl resulted in unreliable peak integration when using 3 and 5 s relaxation delays. The Glu γ_H resonance is most prominent at low pH and low temperature (Figure 5), nearly disappearing into the noise at high temperature and high pH.

In PLGA, the Glu *γ* resonance shifts between 31.0 ppm for the protonated helical conformation and 33.2 ppm for the deprotonated random coil conformation.[19] The presence of both peaks in the ^{13}C spectra (Figure 5) suggests that two populations of side chains are present at 25 °C.

Nuclear Magnetic Resonance Relaxation. The measurement of the spin−lattice relaxation time (T_1), the spin−spin relaxation time (T_2), and the nuclear Overhauser effect (NOE) allows the site-specific spectral density function, $J(\omega)$, of a polymer to be sampled at specific frequencies. When dominated by the dipole−dipole relaxation mechanism,[20] the measurement of T_1 samples the spectral density function at three different frequencies (ω_C, ω_{H+C}, ω_{H-C}):[21]

$$\frac{1}{T_1} = \frac{N}{10}\left(\frac{\mu_0 h \gamma_H \gamma_C}{8\pi^2 r_{CH}^3}\right)^2 (J(\omega_{H-C}) + 3J(\omega_C) + 6J(\omega_{H+C})) \quad (1)$$

where N is the number of attached protons, h is Planck's constant, μ_0 is the permeability of free space, γ_C is the gyromagnetic ratio for carbon, γ_H is the gyromagnetic ratio for protons, r_{CH} is the distance between the carbon and directly bonded proton (1.09 Å), and $J(\omega_X)$ is the value of the spectral density function at a frequency ω_X.

The data show several trends (Figures 6 and 7). The T_1 values increase with increasing temperature. The carbons farther out on the side chain exhibit longer T_1's, with the exception of the *β* carbons that have T_1 values shorter than those for the α carbons. Error bars are

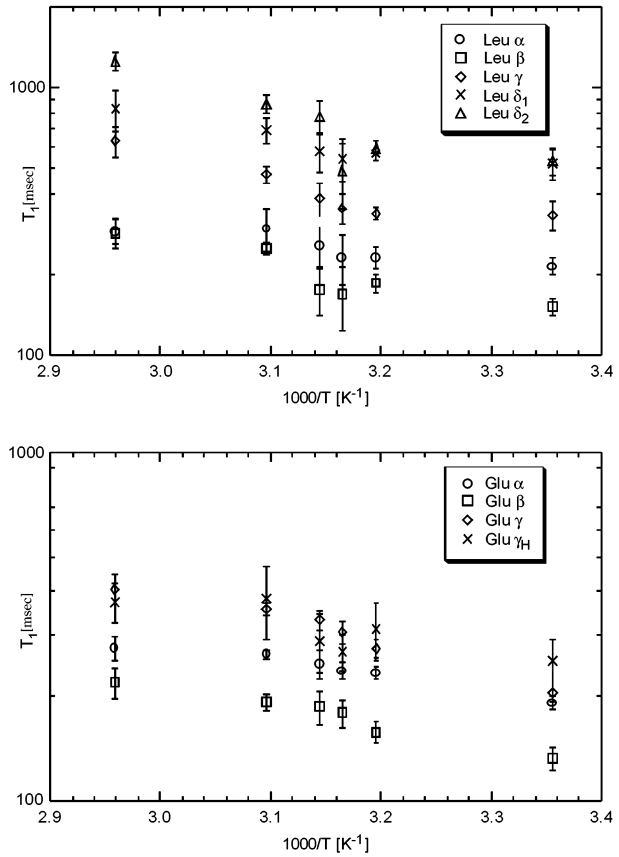

Figure 6. T_1 vs inverse temperature for PEL in pH 4.58 buffer.

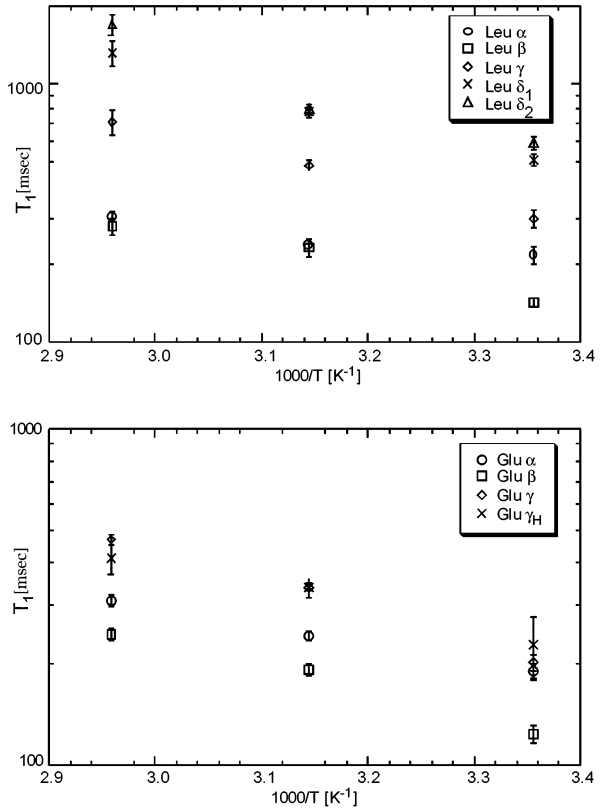

Figure 7. T_1 vs inverse temperature for PEL in pH 7.10 buffer.

calculated from the multiple runs and from the error for the best fit of the inversion−recovery data. Smaller

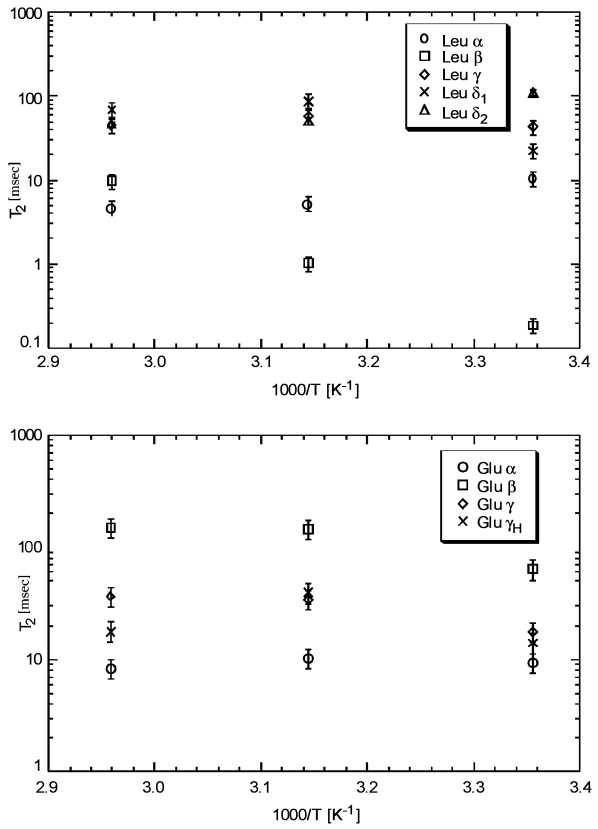

Figure 8. T_2 vs inverse temperature for PEL in pH 4.58 buffer.

peak intensities for the leucine resonances resulted in larger error bars.

When dominated by the dipolar mechanism, the spin−spin relaxation (T_2) is defined as[21]

$$\frac{1}{T_2} = \frac{N}{20}\left(\frac{\mu_0 h \gamma_H \gamma_C}{8\pi^2 r_{CH}^3}\right)^2 (4J(0) + J(\omega_{H-C}) + 3J(\omega_C) + 6J(\omega_{H+C}) + 6J(\omega_H)) \quad (2)$$

where T_2 is the spin−spin relaxation time and all other parameters are defined with eq 1.

Figures 8 and 9 show spin−spin relaxation times calculated from the integral of the resonances, with error bars estimated at 20%.[22] The α carbon relaxation times are very close to one another but decrease slightly with increasing temperature. In the low-pH system, the relaxation times of the glutamic acid resonances increase with temperature, except for Glu γ_H, which shows no trend. The leucine β and $\delta 1$ resonances relax more slowly as temperature increases, while the Leu γ resonance shows no trend and the Leu δ_2 relaxation time decreases with increasing temperature. In the high-pH system, the leucine β, δ_1, and δ_2 relaxation times increase with temperature, while the γ resonance shows no trend. The glutamic acid γ_H and β resonances have relaxation times that decrease with increasing temperature, while the Glu γ resonance shows no trend.

The final parameter measured in this suite of experiments is the nuclear Overhauser effect (NOE). The measured enhancement when the carbon resonance is dominated by dipole−dipole relaxation is[21]

$$\mathrm{NOE} = 1 + \frac{\gamma_H}{\gamma_C}\left(\frac{6J(\omega_{H+C}) - J(\omega_{H-C})}{J(\omega_{H-C}) + 3J(\omega_C) + 6J(\omega_{H+C})}\right) \quad (3)$$

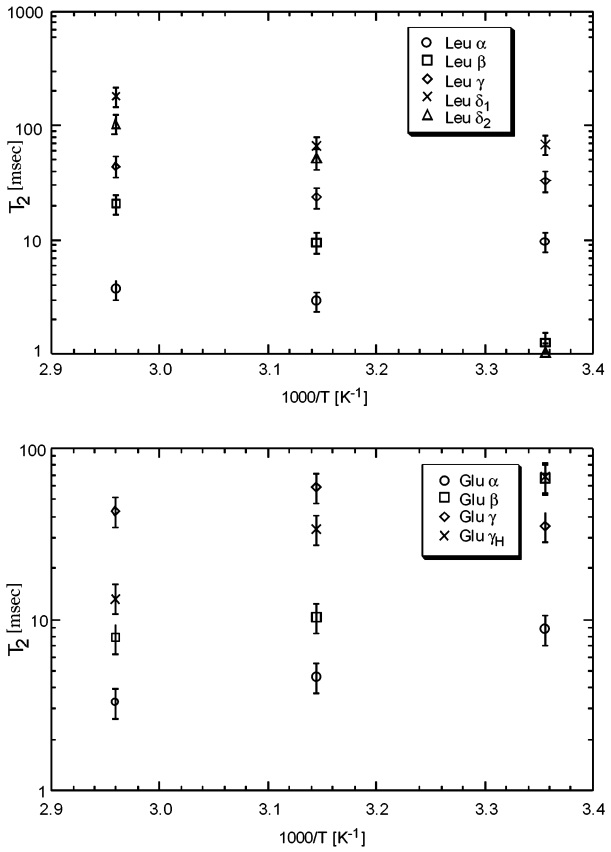

Figure 9. T_2 vs inverse temperature for PEL in pH 7.10 buffer.

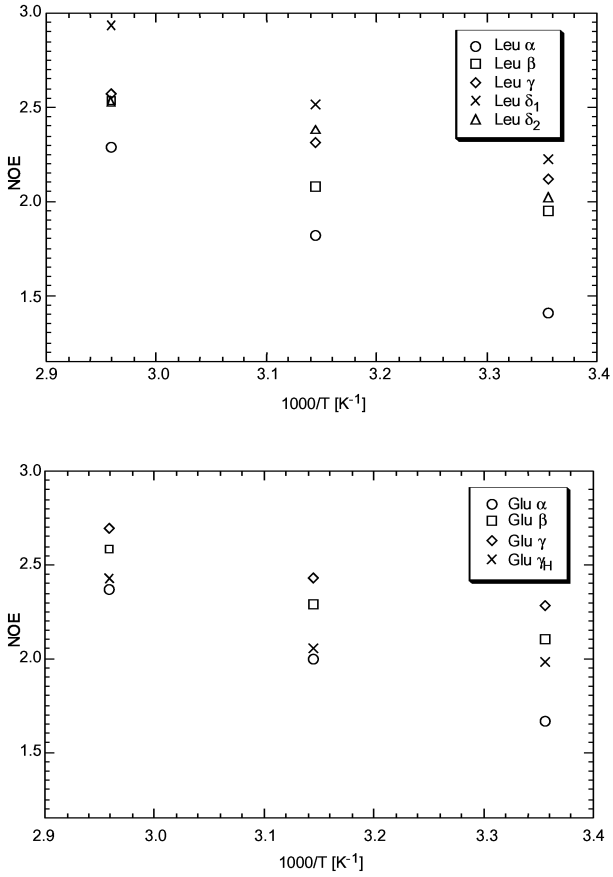

Figure 10. NOE vs inverse temperature for PEL in pH 4.58 buffer.

where NOE is determined as described in the Experimental Section. The data are shown in Figures 10 and 11; they exhibit a monotonic increase with temperature.

Spin−lattice, spin−spin, and NOE parameters were measured for PEL in buffered solution at pH 4.58 and pH 7.10 and at 25, 45, and 65 °C. The data were compared to predicted values based on different model spectral density functions. This was done by minimizing the function[23]

$$E = \left(\frac{T_{1,c} - T_{1,e}}{T_{1,c}}\right)^2 + \left(\frac{T_{2,c} - T_{2,e}}{T_{2,c}}\right)^2 + \left(\frac{\mathrm{NOE_c} - \mathrm{NOE_e}}{\mathrm{NOE_c}}\right)^2 \quad (4)$$

where the c subscript represents calculated values and the e subscript represents experimental values. Several model spectral density functions were selected, as discussed later. The fits were performed in Mathematica, with initial guesses for adjustable parameters varied over several orders of magnitude when necessary.

Nuclear Magnetic Resonance Relaxation Models. The first spectral density function used to model the data is a single correlation time model. This corresponds to an autocorrelation function with a single-exponential decay:[24]

$$G(t) = \exp[-t/\tau_c]; \quad J(\omega) = \frac{2\tau_c}{1 + \omega^2 {\tau_c}^2} \quad (5)$$

Here τ_c is the correlation time, t is time, and ω is frequency. This spectral density function is associated with a hard sphere undergoing isotropic rotational diffusion on a time scale of τ_c. Although polymers undoubtedly experience more complex motions, this model, nevertheless, provides some insight into polymer motions. Reported in Table 3 are the correlation times extracted from the data using eqs 1−5 for the α carbons. These carbons are along the backbone of the chain and are expected to have their motions dominated by the overall global rotation of the polymer globule and local segmental motions. Side chain carbons likely experience the global rotation convoluted with complex internal motions.[25] Within the context of this model, the α carbons exhibit slower motion as temperature is increased. This is likely the result of the polymer globule size increasing as the temperature increases, which results in an increase of the overall rotational correlation time. The Glu α carbon shows slower motion in the high-pH system than in the low-pH system. This is consistent with the intrinsic viscosity results, which show that the polymer globule size will increase with increasing temperature.

Another method to measure the overall rotational correlation time is by using the ratio T_1/T_2. For small molecules this ratio is unity; for polymeric molecules, however, the ratio is proportional to the square of the rotational correlation time, τ_c.[26] Using this ratio partially cancels out the effects of the local motions of the polymer chain and, for the backbone carbons, is likely to give the best results because they experience less local motion than the side chain carbons. Application of this method is also reported in Table 3.

The most common spectral density function used in the study of biopolymers is the "model-free" approach of Lipari and Szabo.[27] This model treats the motion of

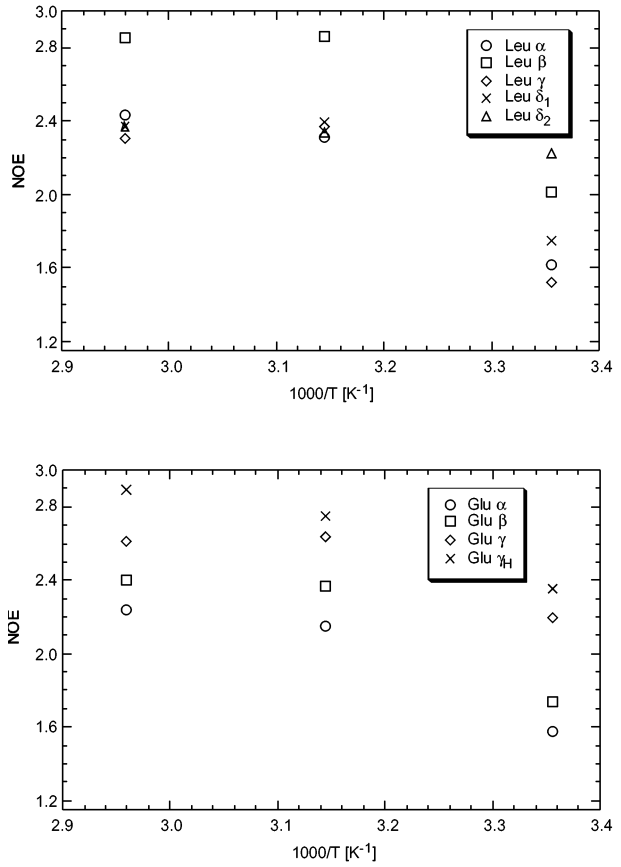

Figure 11. NOE vs inverse temperature for PEL in pH 7.10 buffer.

Table 3. Single Correlation Times Extracted for the α Carbons of Glutamic Acid and Leucine

	Glu α ratio[b,c]		Glu α BF[a]		Leu α ratio		Leu α BF	
pH	4.58	7.10	4.58	7.10	4.58	7.10	4.58	7.10
298 K	12.1	12.0	12.0	12.4	10.5	11.8	12.1	12.7
318 K	13.4	22.7	13.1	19.6	17.8	28.5	18.9	24.5
338 K	15.7	32.3	15.5	26.3	21.7	52.2	21.5	21.5

[a] Best fit method (BF). [b] Ratio method (ratio). [c] Correlation times are reported in nanoseconds.

the internuclear vector as the sum of two motions: the first is the overall rotation of the molecule, characterized by the overall rotational correlation time τ_R; the second is the result of internal motions (such as rotations around a bond, hopping between sites, or restricted diffusion) and is characterized by the internal correlation time, τ_e. In practice, the model treats the motions as uncorrelated; therefore, the method works best if the two correlation times are separated by at least an order of magnitude, preferably two,[28] allowing for the effective decoupling of the motions. The spectral density function is[27]

$$J(\omega) = 2\left(\frac{S^2\tau_R}{1+\omega^2{\tau_R}^2} + \frac{(1-S^2)\tau}{1+\omega^2\tau^2}\right) \qquad (6)$$

where $\tau^{-1} = {\tau_R}^{-1} + {\tau_e}^{-1}$, and S^2 is an order parameter constrained between 0 and 1, which parses the motion into these two modes. With this model, the overall rotational correlation time is usually provided from other methods, such as intrinsic viscosity measurements, or the correlation times extracted from the single

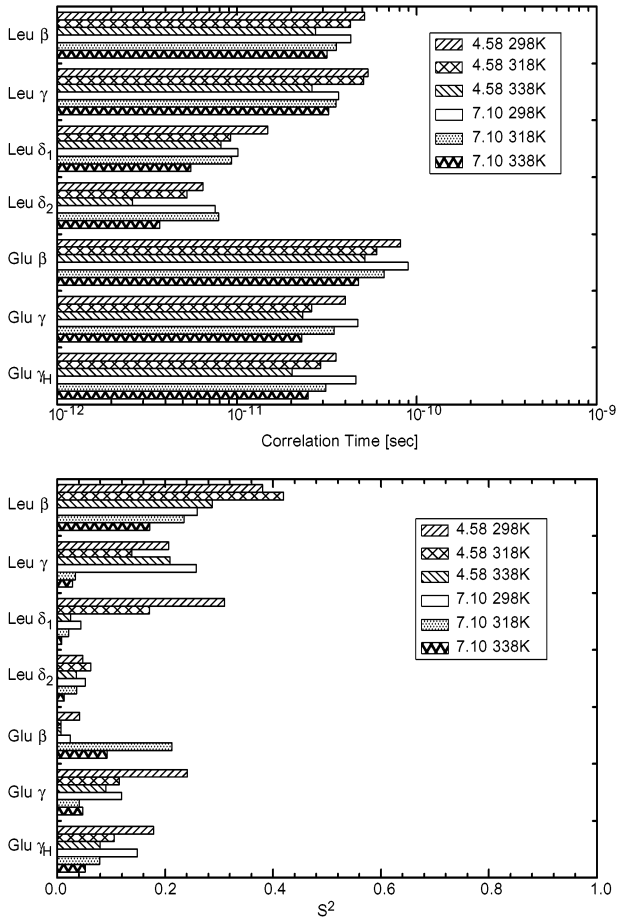

Figure 12. Extracted parameters from the Lipari−Szabo model-free analysis.

correlation time model for the backbone carbons. We use the latter time extracted for the Glu α carbons. The resulting Lipari−Szabo model correlation times for the side chain resonances display a decrease in correlation time with increasing temperature (Figure 12). For most resonances the order parameter decreases with increasing temperature. There is very little change for the Leu γ resonance in the low-pH system.

The order parameter in the model-free formalism can be interpreted in terms of the type of motion expected at different locations in the backbone and on the side chains. For resonances far out on the side chain, the motion of the internuclear vector is the result of the motion about all the bonds between it and the backbone. These multiple degrees of freedom result in a motion that can be modeled as diffusion on a cone of half angle θ[29]

$$S^2 = \left(\frac{(1-\cos\theta)\cos\theta}{2}\right)^2 \qquad (7)$$

Cone angles derived from the order parameters and eq 7 for the γ and δ carbons are shown in Figure 13. The angles are found to be smaller at lower temperatures and pHs. Of particular interest are the Leu γ and Leu δ_1 residues, which show significantly restricted motion at low pH compared to their behavior at high pH.

The motions of theβ carbons can be described as undergoing two-site hopping between two of the three expected rotamers. The third rotamer about the α−β bond is forbidden in the helix conformation for steric

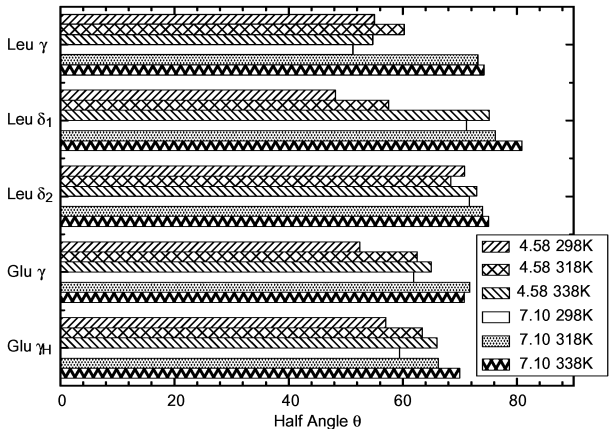

Figure 13. Interpretation of the Lipari−Szabo order parameter in terms of restricted diffusion in a cone of half angle θ, shown for the γ and δ carbon resonances.

Table 4. Ratio of the Populations of Two Sterically Allowed Rotamers of the β Carbons

	Glu β carbon		Leu β carbon	
pH	4.58	7.10	4.58	7.10
298 K	1.55	1.48	3.66	2.68
318 K	1.41	2.39	4.07	2.52
338 K	1.41	1.76	2.88	2.15

reasons.[30] Assuming hopping between the two allowed rotamers, the order parameter is given by[31]

$$S^2 = 1 - \left(\frac{8r}{3(1+r)^2}\right) \tag{8}$$

where r is the ratio of the relative populations of the two states p_1/p_2. The ratios are derived from the S^2 results and are reported in Table 4. The analysis shows that the Leu β rotamers are farther from degeneracy than the Glu β carbon, supporting the hypothesis that at high pH the Leu β carbons experience increased motion vis-à-vis the low-pH data.

Discussion

The intrinsic viscosity data demonstrate that PEL undergoes a pH-mediated collapsing transition from 6.8 nm at a pH of 6.82 to 2.6 nm at a pH 4.92. The intrinsic viscosity of PEL in a random coil conformation compares well with PLGA in 1 M NaCl; however, our data were obtained in 0.2 M KCl. Given that the size of polyelectrolytes is known to decrease with increasing salt concentration,[32] we conclude that the random coil conformation of PEL is likely to be smaller than that of PLGA at a similar ionic strength. This may be attributed to PEL's apparent decrease in charge density, owing to its hydrophobic moieties compared to PLGA. In addition, at low pH the radius of gyration extracted from intrinsic viscosity is much smaller than that observed for a helical rod of PLGA[30,33] and is close to that of a native protein. We conclude that the collapsed form of PEL does not have a rigid-rod helical conformation; rather, the chain consists of helical regions interspersed with nonhelical regions, thus allowing a well-packed globule to form.

The circular dichroism results demonstrate that PEL undergoes a helix−coil transition at a pH of 5.83. Yet, the chemical shifts of PEL do not exhibit the same shifts as PLGA when it undergoes the same transition.[16] The previous studies of PLGA were carried out in low-ionic strength solution where the helix−coil transition occurs very close to the pK_a of the side chain. In our work, the screening of the electrostatic repulsion of the side chain carboxylates allows the helix to persist to high pHs; therefore, the side chains are unprotonated in both the helix and coil states. Interestingly, a resonance for the Glu γ carbon of a protonated side chain is observed (Figure 5), and its shift is not the expected average of protonated and unprotonated chemical shifts. This would imply that the dynamic equilibrium that would occur for an exposed side chain (fast on NMR time scales) is not occurring. Therefore, we surmise that some of the glutamic acid side chains are not accessible to the solvent or have significantly different apparent pK_a values. This may be the result of sequestering in a globule core (the case of inaccessibility) or the close proximity of some carboxyl side chains leading to a shift of the effective pK_a.[34] In fact, a shift in the apparent pK_a of PLGA has been observed using potentiometric titration.[8] The observed reduced intensity of the protonated Glu γ resonance at high temperature (Figure 5) indicates that more of the side chains are able to become deprotonated as a result of the globule-to-coil transition; yet the observation of the protonated resonance at high pH indicates that the system is not completely described as a random coil. This is supported by the CD results that reveal 20% helical character for PEL at a pH of 7.10.

NMR relaxation measurements are capable of providing insight into both the global motion of the polymer chain and the local motions of individual carbon atoms on the residues. The backbone carbons are expected to have their motion dominated by the overall global rotation of the polymer globule with smaller contributions from the internal motion. Using intrinsic viscosity measurements of size, we would expect global rotation times of 18.0 ns for the pH 4.58 sample at 25 °C and 300 ns for the pH 7.10 sample at 25 °C. The correlation times extracted from the NMR data are shorter. This is the result of the sensitivity of NMR to local and segmental motions. Both the single correlation time model and the ratio method exhibit correlation times that become slower with increasing temperature; this is attributed to the change in the size of the polymer globule. The differences between the best fit to the single correlation time model and the ratio method indicate partial canceling of some of the internal motion at high temperature for the high-pH system where the differences in the two methods are most pronounced. The similarities of the two methods at low pH indicate smaller amounts of internal motions that can be canceled by using the ratio method. PEL exhibits higher backbone mobility in the coil state, but not to the extent measured in helix−coil transitions of homopolymers such as poly(γ-benzyl L-glutamate) in organic solvents[35] in which the difference in the backbone correlation times was found to be greater than an order of magnitude. This may be the result of the hydrophobic residues' influence on PEL, preventing both the formation of a rigid-rod-like α-helix and the formation of a completely open random coil at low temperatures.

We expect that the local motions of the β carbons are dominated by the rotations about the α−β bond. The β resonances exhibit a decrease in the correlation time with an increase in temperature. The Lipari−Szabo analysis results in very low order parameters for the Glu β carbon. On the other hand, the Leu β carbon is

best described by an order parameter that is high at low pH and decreases with increasing temperature. In the helical state, it has been demonstrated that only two of the three rotamers are allowed.[30] Using this model for both the helix and coil conformations, the energies of the two rotamers for Glu β are very close to one another, as calculated by the ratio of the populations of the two states. For the Leu β resonance, the two states show a large energy difference at low pH and a smaller, but significant, energy difference at high pH.

The γ carbons are described by motions faster than β carbons. This is expected as they are more removed from the backbone and have motions that are the result of the global rotation of the molecule, the internal motions of the backbone, and rotations about the $\alpha-\beta$ and $\beta-\gamma$ bonds. The convolution of all these motions allows the motion to be well described by restricted diffusion on a cone, with the half angle of the cone determined from the order parameter of the Lipari−Szabo model. In the Glu residues, we observe more restricted movement for low pH than for high pH. The internal correlation time decreases with increasing temperature and shows little effect from the change in pH. The Lipari−Szabo model returns order parameters that are slightly larger at low pH for the protonated Glu γ_H carbons that can be interpreted as slightly restricted motion at low pH. The internal correlation times are slightly faster at low pH. The Leu γ carbon displays larger order parameters at low pH than high pH. This is interpreted as limited motion at low pH. The internal correlation time of this carbon also exhibits a decrease with an increase in pH.

The Leu δ methyl carbons exhibit the fastest internal correlation times on the polymer. For both carbons, the correlation times become faster with increasing temperature. Leu δ_1 exhibits a decrease of the Lipari−Szabo order parameter with an increase in pH, which is interpreted as a restriction of the motion at low pH. The Leu δ_2 resonance does not display a change in the restriction of the motion when the pH is changed.

Conclusions

We have used intrinsic viscosity, circular dichroism, and nuclear magnetic resonance to explore the phase transitions of a commercial random copolymer. IV and CD provide structural information on the size and conformation of the polymer, while NMR probes the local and segmental motion of the polymer in its different phases.

We have demonstrated that PEL undergoes a transition between a collapsed helical globule-like state and an uncollapsed random coil state. The motions of the backbone and leucine side chains display an increase in the internal motion as the system moves from the helical collapsed state to the open random coil state. In particular, the change in the onset of the local motion of the Leu α and Leu β carbons demonstrates this well. The change in the effective pK_a of a certain percentage of the glutamic acid residues also supports the compact globule hypothesis. The differences in the motion indicate movement from the coil phase to the random globule phase (Figure 14); however, full-chain scale freezing of the entire ensemble is not observed.

We surmise that we may be witnessing freezing on smaller length scales. This is supported by the small population of nonexchanging protonated glutamic acid side chains and the changes in the types of motion experienced by the Leu α and Leu β carbons. This localized freezing may be part of a broader phase transition. Additionally, we could be observing an average between a population of frozen chains and a population of unfrozen chains, where the unfrozen chains consist of exchanging glutamic acid side chains and the frozen chains contribute to both the exchanging and nonexchanging Glu γ peaks. Further experimental studies focusing on the effects of temperature, degree of heterogeneity, and molecular weight would clarify the phase behavior of these systems.

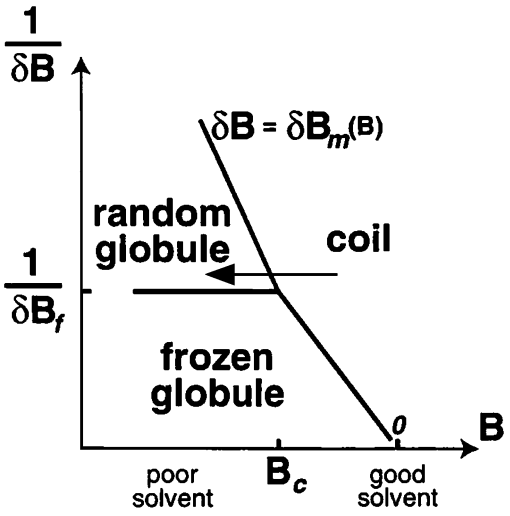

Figure 14. Phase diagram due to Pande et al.[1] B is the second virial coefficient, which is a measure of solvent quality. $1/\delta B$ is the inverse of the standard deviation of the distribution of the second virial coefficients of the monomers along the chain. The arrow depicts the proposed movement on the phase diagram from a pH of 7.10 to a pH of 4.58.

Acknowledgment. This work was supported in part by the Director, Office of Energy Research, Office of Basic Energy Science, Materials Science Division, U.S. Department of Energy, under Contract DE-AC03-76SF00098.

References and Notes

(1) Pande, V. S.; Grosberg, A. Y.; Tanaka, T. *J. Chem. Phys.* **1997**, *107*, 5118.
(2) Sfatos, C. D.; Gutin, A. M.; Shakhnovich, E. I. *Phys. Rev. E* **1993**, *48*, 465.
(3) Bryngelson, J. D.; Wolynes, P. G. *Proc. Natl. Acad. Sci. U.S.A.* **1987**, *84*, 7524.
(4) Bryngelson, J. D.; Onuchic, J. N.; Socci, N. D.; Wolynes, P. G. *Proteins: Struct., Funct., Genet.* **1995**, *21*, 167.
(5) Mazur, J.; McIntyre, D. *Macromolecules* **1975**, *8*, 464.
(6) Cunibert, C.; Bianchi, U. *Polymer* **1974**, *15*, 346.
(7) Bychkova, V. E.; Semisotnov, G. V.; Ptitsyn, O. B.; Gudkova, O. V.; Mitin, Yu. V.; Anufrieva, E. V. *Mol. Biol.* **1980**, *14*, 215.
(8) Anufrieva, E. V.; Bychkova, V. E.; Krakovyak, M. G.; Pautov, V. D.; Ptitsyn, O. B. *FEBS Lett.* **1975**, *55*, 46.
(9) Bychkova, V. E.; Gudkov, A. T.; Miller, W. G.; Mitin, Yu. V.; Ptitsyn, O. B.; Shpungin, I. L. *Biopolymers* **1975**, *14*, 1739.
(10) Semisotnov, G. V.; Zikherman, K. Kh.; Kasatkin, S. B.; Ptitsyn, O. B.; Anufrieva, E. V. *Biopolymers* **1981**, *20*, 2287.
(11) Karnoup, A. S.; Uversky, V. N. *Macromolecules* **1997**, *30*, 7427.
(12) Meiboom, S.; Gill, D. *Rev. Sci. Instrum.* **1958**, *29*, 688.
(13) Tanford, C. *Adv. Protein Chem.* **1968**, *23*, 121.
(14) Einstein, A. *Ann. Phys.* **1906**, *19*, 289.
(15) Wüthrich, K. *NMR of Proteins and Nucleic Acids*; John Wiley & Sons: New York, 1986.
(16) Rance, M.; Sorensen, O. W.; Bodenhausen, G.; Wagner, G.; Ernst, R. R.; Wüthrich, K. *Biochem. Biophys. Res. Commun.* **1983**, *117*, 479.
(17) Howarth, O. W.; Lilley, D. M. J. *Prog. NMR Spectrosc.* **1978**, *12*, 1.
(18) Morris, G. A.; Hall, L. D. *J. Am. Chem. Soc.* **1981**, *103*, 4703.

(19) Lyerla, J. R., Jr.; Barber, B. H.; Freedman, M. H. *Can. J. Biochem.* **1973**, *51*, 460.
(20) Peng, J. W.; Wagner, G. *Methods Enzymol.* **1994**, *239*, 563.
(21) Abragam, A. *Principles of Nuclear Magnetism*; Clarendon Press: Oxford, England, 1961.
(22) Tylianakis, E. I.; Dais, P.; Heatly, F. *J. Polym. Sci., Part B: Polym. Phys.* **1993**, *35*, 317.
(23) Dello, M. J.; Wand, A. J. *J. Am. Chem. Soc.* **1989**, *111*, 4571.
(24) Howarth, O. W. In *NMR Spectroscopy of Polymers*; Ibbett, R. N., Ed.; Blackie Academic and Professional: New York, 1993.
(25) Hanssum, H.; Rüterjans, H. *J. Chem. Phys.* **1983**, *78*, 4687.
(26) Arvidsson, K.; Jarvet, J.; Allard, P.; Ehrenberg, A. *J. Biomol. NMR* **1994**, *4*, 653.
(27) Lipari, G.; Szabo, A. *J. Am. Chem. Soc.* **1982**, *104*, 4546.
(28) Lipari, G.; Szabo, A. *J. Am. Chem. Soc.* **1982**, *104*, 4559.
(29) Palmer, A. G., III.; Williams, J.; McDermott, A. *J. Phys. Chem.* **1996**, *100*, 13293.
(30) Hahn, U.; Hanssum, H.; Rüterjans, H. *Biopolymers* **1985**, *24*, 1147.
(31) Torchia, D. A.; Nicholson, L. K.; Cole, H. B. R.; Kay, L. E. In *NMR of Proteins*; Clore, G. M., Gronenborn, A. M., Eds.; CRC Press: Boca Raton, FL, 1993.
(32) Higgs, P. G.; Joanny, J.-F. *J. Chem. Phys.* **1991**, *94*, 1543.
(33) Bychkova, V. E.; Ptitsyn, O. B.; Barskaya, T. V. *Biopolymers* **1971**, *10*, 2161.
(34) Blanch, H. W.; Clark, D. S. *Biochemical Engineering*; Marcel Dekker: New York, 1996.
(35) Allerhand, A.; Oldfield, E. *Biochemistry* **1973**, *12*, 3428.

MA021433K